Hindawi
Mathematical Problems in Engineering
Volume 2022, Article ID 5013146, 17 pages
https://doi.org/10.1155/2022/5013146

Research Article

Parameter Estimation of Solar PV Using Ali Baba and Forty Thieves Optimization Technique

Pankaj Sharma,[1] **Saravanakumar Thangavel**,[1] **Saravanakumar Raju**,[1] **and B. Rajanarayan Prusty**[2]

[1]*School of Electrical Engineering, Vellore Institute of Technology, Vellore, India*
[2]*Department of Electrical and Electronics Engineering, Alliance College of Engineering and Design, Alliance University, Bengaluru, India*

Correspondence should be addressed to B. Rajanarayan Prusty; b.r.prusty@ieee.org

Received 25 August 2022; Revised 30 October 2022; Accepted 13 December 2022; Published 29 December 2022

Academic Editor: Zhiwen Chen

The modeling of a solar PV system is challenging due to its nonlinear current vs. voltage characteristics. Although various optimization techniques have been applied for the parameter estimation of the solar PV system, there is still a scope to attain the best-optimized results. This paper uses a new meta-heuristic optimization algorithm and a classical technique named Ali Baba and the Forty Thieves (AFT) with Newton Rapson (NR) method to estimate solar PV system parameters. The well-known story of Ali Baba and the Forty Thieves has inspired the AFT. Besides, the inappropriate objective function used in earlier research to extract parameters from solar PV models is recognized. The experimental findings demonstrate that the suggested approach performs better when compared to state-of-the-art algorithms. Between the measured data and the computed data for AFT, the root mean square error values for the five PV models, such as single diode model (SDM), double diode model (DDM), Photowatt-PWP201, STM6-40/36, and STP6-120/36, are respectively $7.72 \times 10^{-04} \pm 6.121 \times 10^{-16}$, $7.412 \times 10^{-04} \pm 9.52 \times 10^{-06}$, $2.052 \times 10^{-03} \pm 3.05 \times 10^{-17}$, $0.001721922 \pm 2.19 \times 10^{-17}$, and $0.014450817 \pm 3.42 \times 10^{-16}$. In terms of accuracy, the obtained results indicate that the proposed AFT algorithm is more efficient than the other optimization techniques available in the literature. The excellent correlation between the estimated parameters from characteristic curves and observed data for SDM, DDM, Photowatt-PWP201, STM6-40/36, and STP6-120/36 demonstrates that the proposed AFT is a potential option among the techniques available in the literature. The Friedman and Wilcoxon tests have been used to assess the statistical validity of the proposed algorithms.

1. Introduction

Various environmental and energy-related considerations have contributed to the increased use of alternative energy sources. In recent years, large solar PV plant installations have been used to generate electric power. PV systems are generally installed in open spaces exposed to adverse weather like gales and torrential rain [1, 2]. In response to these challenges, a much more precise information framework is formulated to pinpoint the crucial characteristics of PV systems in the solar sector. Assessments of PV electricity generation, productivity estimations, voltage regulation, MPPT, and better power monitoring of the PV arrays benefit from thoroughly examining PV input parameters retrieval. A mathematical equation is formulated first, followed by determining such variables throughout the detailed modeling of PV systems. The single diode model (SDM) is commonly applied in almost all modeling techniques in all real-world scenarios. Moreover, if such estimates are exposed to contingency system aging, these undefined variables will most likely have an unreliable and failure effect on the characteristics of the PV models. A crucial modeling task is to estimate the PV cell characteristics beforehand accurately. The PV framework is a dynamic system with a nonconvex relation, the solution of which has several problems and obstacles. Researchers and scientists have recently put a

lot of effort into accurately estimating unknown values [3]. The identification of accurate values of such parameters, such as photo current (I_{Ph}), saturated current (I_0), shunt resistance (R_{Sh}), series resistance (R_S), and diode identity factor (N), is essential. Due to solar cells' nonlinear current-voltage (I-V) characteristics, estimating their parameters is considered a nonlinear optimization problem [4].

In the literature, various methods for estimating PV parameters are being used. And these approaches are classified into three groups. They are analytic, determinism, and meta-heuristic (MH) optimization techniques [5]. Analytical techniques calculate factors such as the open-circuit voltage, short-circuit current, MPPT, and I-V characteristics based on the supplier's information. Some of the data sets on the I-V characteristic curve are employed in the analytic method for finding the variables that minimize the discrepancy between the expected and calculated values. The concept of "Using every exact quantitative measurement for a coherent system" underlies deterministic approaches, which recover the independent variables using only a sizable quantity of data [6]. Depending on a differential among practical but estimated data sets, an optimization problem serves as its foundation. Those procedures might have the localized optimal solution since they depend on different parameters. Since they both operate on the principle of "Using every exact value for the complete solution," MH approaches are comparable to deterministic approaches. They are regarded as the world's greatest optimization technique due to their many benefits, including resilience, efficiency, stability, elegance, and easy implementation [7]. There are different literary categories in which MH optimization algorithms have been classified, including swarm, evolutionary, human behavior, and physics-based optimization algorithms. Particle swarm optimization (PSO) [8], simulated annealing (SA) [9], mutative scale parallel chaos optimization (MPCOA) [10], bee pollinator flower pollination algorithm (BPFPA) [11], artificial bee swarm optimization (ABSO) [12], generalized oppositional teaching learning-based optimization (GOTLBO) [13], flower pollination algorithm (FPA) [14], genetic algorithm (GA) [15], harmony search (HS) [16], Levenberg–Marquardt algorithm with SA (LMSA) [17], artificial bee colony optimization (ABCO) [18], artificial immune system (AIS) [19], cuckoo search (CS) [20], honey badger algorithms (HBA) [21], heap-based optimizer (HBO) [22], tree seed algorithm (TSA) [23], ranking-teaching-learning-based optimization (RTLBO) [24], bacterial foraging algorithm (BFA) [25], teaching-learning-based optimization (TLBO) [26], gaining–sharing knowledge (GSK) [27], and whale optimization algorithm (WOA) [28, 29] are few examples of well-known MH algorithms that were developed to evaluate the solar PV system's parameters.

The root mean square error (RMSE) value is used to assess the proposed optimization technique's correctness. Additionally, data from recent MH algorithms are compared to the characteristics obtained from the AFT. All these researches offer an assessment of the suggested algorithm's precision for parameter estimation of solar PV. This study concentrates on SDM, double diode model (DDM), Photowatt-PWP201, STM6-40/36, and STP6-120/36 solar PV models. Temperature and irradiance affect the solar PV model's parameters. Therefore, a reliable parameter estimate is necessary to model solar PV. The proposed algorithm is very efficient for solving nonlinear problems. The famous story of Ali Baba and the Forty Thieves has inspired this algorithm. In the story, Ali Baba witnessed forty criminals enter a mysterious cave brimming with valuables. The performance of the AFT algorithm has been evaluated on a collection of fundamental benchmark test functions, including simple and sophisticated test functions with varied dimensions and levels of complexity. In addition, the AFT algorithm has been subjected to a thorough comparison with other well-researched algorithms, and statistical test techniques have been used to demonstrate the relevance of the findings. This paper's main contribution is as follows:

(1) A new MH optimization algorithm (AFT) is introduced to solve the solar PV parameter extraction

(2) The proposed AFT performance is successfully applied for the SDM, DDM, Photowatt-PWP201, STM6-40/36, and STP6-120/36, with the significant similarity between the simulated and experimental P-V as well as I-V curves, clearly demonstrated

(3) The proposed AFT demonstrates superiority by achieving the lowest RMSE objectives

(4) The result of the AFT with other MH optimization techniques is compared

This paper is organized as follows: Section 2 illustrates the solar PV models such as SDM and DDM. Section 3 explains AFT comprehensively. The objective function is presented in Section 4. Section 5 lucidly presents the results and critically discusses the inferences considering five PV modules: SDM, DDM, Photowatt-PWP201, STM6-40/36, and STP6-120/36. Statistical validations (Friedman and Wilcoxon test) are presented in Section 6. And the final section summarizes the concluding remarks and the future scope of the paper.

2. Solar PV Models

This section elaborates on SDM and DDM comprehensively.

2.1. Single-Diode Model (SDM). Several equivalent circuits have been developed to illustrate the I-V characteristics of PV modules. The SDM is the most widely utilized PV equivalent circuit model. SDM is simple and incredibly accurate [30, 31]. It is the most famous mathematical concept, but as its title indicates, it establishes the relationship among the variables using a single-diode approximation [32]. I is the output current, I_{Sh} is the shunt resistance current, R_s is the series resistance, I_{Ph} is the photocurrent, I_D is the diode current, and R_{Sh} is the shunt resistance [33, 34], as shown in Figure 1.

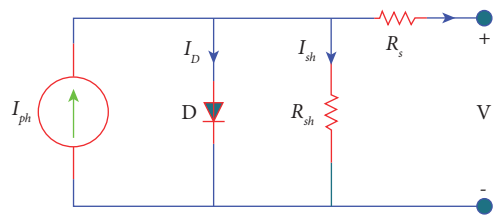

Figure 1: Equivalent circuit for SDM.

$$I = I_P - I_D - I_{\text{Sh}}. \tag{1}$$

The mathematical equations for the I_D and I_{sh} are given by equations (2) and (3), respectively.

$$I_D = I_{sd}\left(e^{(qV_L+IR_s/n\text{KT})} - 1\right), \tag{2}$$

$$I_{\text{sh}} = \frac{V_L + IR_s}{R_{\text{sh}}}, \tag{3}$$

$$I = I_{\text{sd}}\left(e^{(q(V_L+IR_s/n\text{KT})-} 1\right)^{-} \frac{V_L + IR_s}{R_{\text{sh}}}. \tag{4}$$

The PV module output current is given by the following equation:

$$I = I_{\text{ph}}N_p - I_{\text{sd}}N_p\left[e^{\left(V_L+\text{I}R_sN_s/N_p/nN_sV_t\right)} - 1\right] - \frac{V_L + \text{I}R_sN_s/N_p}{R_{\text{sh}}N_s/N_p}, \tag{5}$$

where $q = 1.6021764 \times 10^{-19}$, Boltzman constant ($K$), temperature ($T$), N_p, and N_s, respectively, are the number of cells in parallel and series, and the diode ideality factor is n. These parameters (I_{Ph}, I_o, R_{sh}, R_s, and N) can be extracted to determine an accurate PV model [35].

2.2. Double-Diode Model (DDM). Since the SDM excludes the effect of recombining energy loss in circuitry, the loss problem is solved by employing the more precise model DDM [30]. The circuit diagram of DDM is shown in Figure 2.

The current I flows through the DDM circuit can be computed as follows:

$$I = I_P - I_{\text{sh}} - I_{D1} - I_{D2}, \tag{6}$$

where I_{D1} is the first diode's current and I_{D2} is the second diode's current.

$$I_{D1} = I_{o1}\left(e^{((V_L+IR_s/n_1V_t)} - 1\right), \tag{7}$$

$$I_{D2} = I_{o2}\left(e^{((V_L+IR_s/n_2V_t)} - 1\right), \tag{8}$$

where n_1 and n_2 are the ideal factor of the diode. From (6) and (7), I can be computed as

$$I = I_{\text{ph}}^{-}I_{o1}\left(e^{((V_L+IR_s/n_1V_t)} - 1\right) - I_{02}\left(e^{((V_L+IR_s/n_2V_t)} - 1\right) - \frac{V_L + \text{I}\,R_s}{R_{\text{sh}}}. \tag{9}$$

These parameters (I_{Ph}, I_{01}, I_{02}, R_{Sh}, R_s, N_1, and N_2) can be extracted from DDM.

3. Ali Baba and Forty Thieves (AFT) Optimization Technique

This work's main objective is to apply an optimization technique that uses the story of Ali Baba and the Forty Thieves as unified modeling of human social interaction. The primary presumptions of this method are satisfied by the concepts that follow, which are drawn by this story [36]:

(i) To locate Ali Baba's home, the forty thieves work together as a team to receive directions to someone or another thief. As a result, such data may be inaccurate

(ii) From an initial position, the forty thieves will travel a range till they reach Ali Baba's house

(iii) Marjaneh may fool her robber's several ways by using cunning techniques to keep Ali Baba partially protected from their approach

It is possible to connect the actions of Marjaneh and the robbers to an objective function that needs to be optimized. This allows the development of the new MH method described as follows.

3.1. Random Initialization. The AFT process is started by initializing n people's position in such a d-dimensional state space at random, as given as follows:

$$x = \begin{bmatrix} x_1^1 & x_2^1 & x_3^1 & \dots & x_d^1 \\ x_1^2 & x_2^2 & x_3^2 & \dots & x_d^2 \\ x_1^n & x_2^n & x_3^n & \dots & x_d^n \end{bmatrix}, \tag{10}$$

where x = position of all thieves, d = number of variables of a given problem, and $x_j^i = j$th dimension of the ith thief.

Marjaneh's wit ranking concerning all thieves could be initiated as follows:

$$m = \begin{bmatrix} m_1^1 & m_2^1 & \dots & m_d^1 \\ m_1^2 & m_2^2 & \dots & m_d^2 \\ m_1^n & m_2^n & \dots & m_d^n \end{bmatrix}, \tag{11}$$

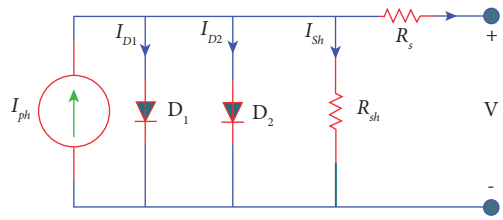

Figure 2: Equivalent circuit for DDM.

(1) u_j & l_j are the upper and lower bounds of j^{th} dimension, x is the position, and n is the number of thieves.
(2) Initialization of best (best_t^i) position and global best $(g\text{best})$ position.
(3) Evaluate the fitness function $f(x)$
(4) **set** $t \leftarrow 1$
(5) **while** $(t < T)$ **do do**
(6) $Td_t = 1.0 * e^{-2.0(t/T)^{2.0}}$
(7) $P_{pt} = 0.1 * \log(2.0(t/T)^{0.1})$
(8) **for** $i = 1, 2, \ldots..n$ **do**
(9) **if** $(\text{rand} \geq 0.5)$ **then**
(10) **if** $(\text{rand} \geq P_{pt})$ **then**
(11) $x_{t+1}^i = g\text{best} + [Td_t(\text{best}_t^i - y_t^i)r_1 + Td_t(y_t^i - m_t^{a(i)})r_2]\text{sgn}(\text{rand}-0.5)$
(12) Else
(13) $x_{t+1}^i = Td_t[(u_j^- l_j)\text{rand} + l_j]$
(14) **end if**
(15) $x_{t+1}^i = g\text{best}_t^- [Td_t(\text{best}_t^i - y_t^i)r_1 + Td_t(y_t^i - m_t^{a(i)})r_2]\text{sgn}(\text{rand}-0.5)$
(16) **end if**
(17) **end for**
(18) **for** $i = 1, 2, \ldots., n$ **do**
(19) Check, evaluate and update the new positions
(20) Evaluate and update the solutions for $m_t^{a(i)}$, (best_t^i) & $(g\text{best})$.
(21) **end for**
(22) $t = t + 1$
(23) **end while**

Algorithm 1: The pseudocode of AFT.

where m_j^i = astute level of Marjaneh concerning the ith thief at the jth dimension which indicates Marjaneh's level of intelligence in comparison to the jth dimension's ith thief.

3.2. Fitness Evaluation. A user-defined fitness value that is assessed to every thief's location contains the choice independent variables. The related objective functions are kept in a collection and are presented as follows:

$$f = \begin{bmatrix} f_1 x_1^1 & f_1 x_2^1 & \cdots & f_1 x_d^1 \\ f_2 x_1^2 & f_2 x_2^2 & \cdots & f_2 x_d^1 \\ f_n x_d^n & f_n x_d^n & \cdots & f_n x_d^n \end{bmatrix}, \quad (12)$$

where x_d^n = dimension position of n^{th} thief.

The effectiveness of the response is assessed to every thief's different destination in the AFT technique model using a predefined objective function. If the new destination's solutions performance is higher than the old one, the position is then upgraded. On the other hand, if his present solutions grade is superior to the current one, every thief remains there.

3.3. Proposed Mathematical Model. Three primary cases discussed above may arise. At the same time, robbers look for Ali Baba. Every time, it is assumed that the thieves do thorough searches all through the surroundings. At the same time, a percentage happens due to Marjaneh's cleverness, which compels the robbers to look in unlikely places. Finally, it is earlier looking; the following behavior can be analytically modeled:

Case 1. The robbers might use details they learned from others to find Ali Baba. Under this instance, the robbers' actual places can be discovered as follows:

Table 1: Parameters range of PV models.

Parameters	Single diode		Double diode		STM6-40/36		STP6-120/36		Photowatt-PWP201	
	LB	UB	LB	UB	LB	UB	LB	UB	LB	UB
I_{ph} (A)	0	1	0	1	0	2	0	8	0	2
I_o (μA)/I_{o1} (μA), I_{o2} (μA)	0	1	0	1	0	50	0	50	0	50
I_{Sh} (Ω)	0	0.5	0	0.5	0	0.36	0	0.36	0	2
R_s (Ω)	0	100	0	100	0	1000	0	1500	0	2000
N/N_1, N_2	1	2	1	2	1	60	1	50	1	50

Table 2: Comparison of actual and experimental values for SDM.

S. no	I_m	I_e	IAE (current)	V	P_e	P_m	IAE (power)	RE
1	0.764	0.764149	0.000149	−0.2057	−0.15719	−0.15715	3.07×10^{-05}	−0.0002
2	0.762	0.762702	0.000702	−0.1291	−0.09846	−0.09837	9.06×10^{-05}	−0.00092
3	0.7605	0.761374	0.000874	−0.0588	−0.04477	−0.04472	5.14×10^{-05}	−0.00115
4	0.7605	0.760155	0.000345	0.0057	0.004333	0.004335	1.97×10^{-06}	0.000454
5	0.76	0.759039	0.000961	0.0646	0.049034	0.049096	6.21×10^{-05}	0.001264
6	0.759	0.758011	0.000989	0.1185	0.089824	0.089942	0.000117	0.001303
7	0.757	0.757046	4.57×10^{-05}	0.1678	0.127032	0.127025	7.67×10^{-06}	-6×10^{-05}
8	0.757	0.756085	0.000915	0.2132	0.161197	0.161392	0.000195	0.001209
9	0.7555	0.755022	0.000478	0.2545	0.192153	0.192275	0.000122	0.000632
10	0.754	0.753597	0.000403	0.2924	0.220352	0.22047	0.000118	0.000534
11	0.7505	0.751327	0.000827	0.3269	0.245609	0.245338	0.00027	−0.0011
12	0.7465	0.747305	0.000805	0.3585	0.267909	0.26762	0.000289	−0.00108
13	0.7385	0.740085	0.001585	0.3873	0.286635	0.286021	0.000614	−0.00215
14	0.728	0.727426	0.000574	0.4137	0.300936	0.301174	0.000237	0.000788
15	0.7065	0.707026	0.000526	0.4373	0.309182	0.308952	0.00023	−0.00074
16	0.6755	0.6754	9.97×10^{-05}	0.459	0.310009	0.310055	4.58×10^{-05}	0.000148
17	0.632	0.630998	0.001002	0.4784	0.30187	0.302349	0.000479	0.001585
18	0.573	0.572175	0.000825	0.496	0.283799	0.284208	0.000409	0.00144
19	0.499	0.499539	0.000539	0.5119	0.255714	0.255438	0.000276	−0.00108
20	0.413	0.413485	0.000485	0.5265	0.2177	0.217445	0.000255	−0.00117
21	0.3165	0.317161	0.000661	0.5398	0.171204	0.170847	0.000357	−0.00209
22	0.212	0.212017	1.65×10^{-05}	0.5521	0.117054	0.117045	9.12×10^{-06}	-7.8×10^{-05}
23	0.1035	0.102637	0.000863	0.5633	0.057815	0.058302	0.000486	0.008343
24	−0.01	−0.0093	0.000701	0.5736	−0.00533	−0.00574	0.000402	0.070131
25	−0.123	−0.12436	0.001362	0.5833	−0.07254	−0.07175	0.000794	−0.01107
26	−0.21	−0.2091	0.000898	0.59	−0.12337	−0.1239	0.00053	0.004275
IAE (current)			0.017632		IAE (power)		0.006481	

$$x_{t+1}^{i} = g\text{best} + \left[Td_t\left(\text{best}_t^{i} - y_t^{i}\right)r_1 + Td_t\left(y_t^{i} - m_t^{a(i)}\right)r_2\right]\text{sgn}\left(\text{rand} - 0.5\right); r_3 \geq 0.5, r_4 > P_{pt}. \tag{13}$$

Case 2. The thieves might realize that they have really been misled and begin searching haphazardly about Ali Baba. Throughout this instance, the thieves' actual destinations can be discovered as shown in the following equation:

$$x_{t+1}^{i} = Td_t\left[\left(u_j - l_j\right)\text{rand} + l_j\right]; r_3 \geq 0.5, r_4 \leq P_{pt}. \tag{14}$$

Case 3. This work further analyses the investigation in locations of which some might be found by equation (11) in terms of improving the exploratory and exploitative aspects of the AFT algorithms. In this instance, the thieves' exact location can be discovered as shown in the following equation:

$$x_{t+1}^{i} = g\text{best}_t - \left[Td_t\left(\text{best}_t^{i} - y_t^{i}\right)r_1 + Td_t\left(y_t^{i} - m_t^{a(i)}\right)r_2\right]\text{sgn}\left(\text{rand}^{-} 0.5\right); r_3 < 0.5. \tag{15}$$

Table 3: The IAE, RMSE, and the extracted parameters for SDM.

Sl.no	Optimization techniques	IAE (current)	RMSE			I_{ph}	I_o	R_{Sh}	R_s	N
			Std.	Mean	Min					
1	AFT	0.017632	6.121×10^{-16}	7.72×10^{-04}	7.72×10^{-04}	0.7607	0.3106	52.88991	0.0365	1.4772
2	IWOA [29]	0.0177034	1.1267×10^{-05}	9.952×10^{-04}	9.8602×10^{-04}	0.7608	0.3232	53.7317	0.0364	1.4812
3	GSK [27]	0.0254	2.18×10^{-17}	9.8602×10^{-04}	9.8602×10^{-04}	0.7608	0.3231	53.7227	0.0364	1.4812
4	DE [27]	0.0181	6.72×10^{-05}	1.0096×10^{-03}	9.8602×10^{-04}	0.7608	0.3231	53.7185	0.0364	1.4812
5	RTLBO [24]	0.0217	3.06×10^{-05}	1.0057×10^{-03}	9.8604×10^{-04}	0.7608	0.3423	55.3065	0.0361	1.4871
6	TLABC [40]	0.0203	1.76×10^{-05}	9.9811×10^{-04}	9.8602×10^{-04}	0.7608	0.3231	53.7164	0.0364	1.4812
7	BES [41]	0.0239	2.63×10^{-13}	$9{:}8602\times10^{-04}$	$9{:}8602\times10^{-04}$	0.7607	0.3230	53.7185	0.0364	1.4812
8	HBA [21]	0.0256	7.8106×10^{-10}	9.8602×10^{-04}	9.8602×10^{-04}	0.7608	0.3230	53.7185	0.0364	1.4812
9	HBA-OBL [21]	0.0265	2.2350×10^{-10}	9.8602×10^{-04}	9.8602×10^{-04}	0.7608	0.3230	53.7185	0.0364	1.4812
10	GOTLBO [13]	0.0233	1.36×10^{-04}	1.0949×10^{-03}	9.8760×10^{-04}	0.7608	0.3420	53.8599	0.0362	1.4870
11	HBO [22]	0.0219129	4.0944×10^{-04}	1.5065×10^{-04}	9.8869×10^{-04}	0.76087	0.319	52.15628	0.0364	1.48003
12	WOA [29]	0.0184048	2.2147×10^{-03}	3.0808×10^{-03}	1.0480×10^{-03}	0.7606	0.3881	60.5623	0.0357	1.4999

The iterative procedures provided in the method can be used to simplify the pseudocode of AFT algorithms as discussed in Algorithm 1.

4. Objective Function

The main goal is always to lessen the overall discrepancy between the measured and theoretical findings while evaluating the PV cell characteristics. An objective function called the RMSE can be constructed in a way as to yield the optimal parameters for the PV model's variables [37]. This paper aims to evaluate the characteristics of a PV based on the current and voltage data using MH optimization approaches. The RMSE values between the observed and anticipated actual rates form the basis of the goal function. Two optimization parameters are taken into consideration in this work for evaluating the PV characteristics given in the following equation:

$$F_1 = \sqrt{\frac{1}{N}\left(\left[I_{\text{mes}} - I_{\text{calc}}\right]^2\right)}. \tag{16}$$

The individual absolute error (IAE) of current and power is given in (17) and (18). The relative error (RE) is shown in the following equation:

$$\text{IAE}_{\text{Current}} = \sum_{i=1}^{N} \left|I_{\text{mes}} - I_{\text{calc}}\right|, \tag{17}$$

$$\text{IAE}_{\text{Power}} = \sum_{i=1}^{N} \left|P_{\text{mes}} - P_{\text{calc}}\right|, \tag{18}$$

$$\text{RE} = \frac{I_{\text{mes}} - I_{\text{calc}}}{I_{\text{mes}}}, \tag{19}$$

where I_{mes} is the measured current, I_{calc} is the calculated current, P_{mes} is the measured power, P_{calc} is the calculated current, and N is the number of samples.

The fundamental method for deriving the solar PV model's parameters from observed measurements is to compute the RMSE using the essential functions F_1. The estimated current may be determined by determining the nonlinear formulae. Because this approach requires a lot of calculation, the authors introduced a novel method during which objective function equations roughly estimate the genuine fault. As a result, a solution is used in the first way to calculate the RMSE of the erroneous values [27].

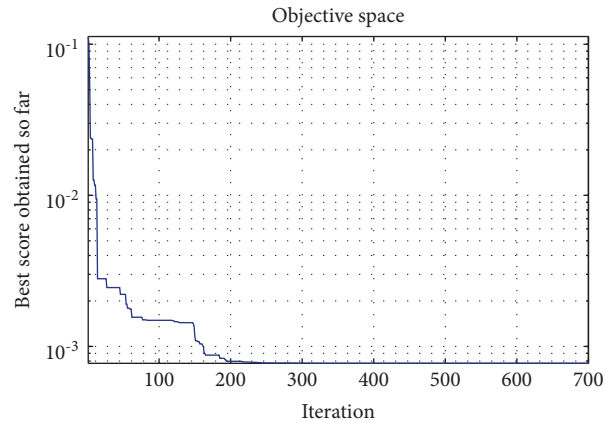

Figure 3: Convergence curve for SDM.

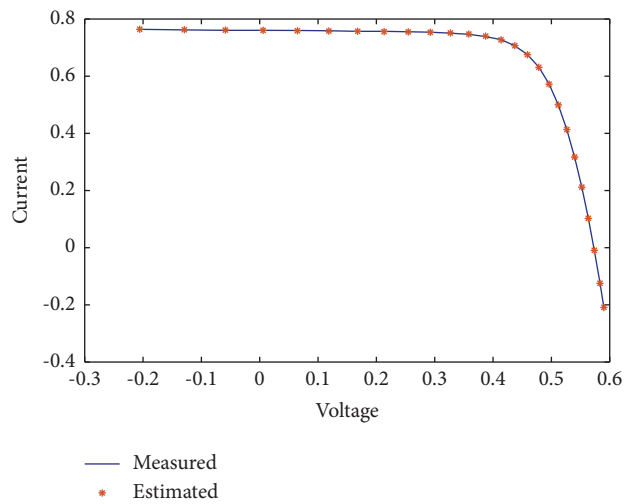

Figure 4: Measured and estimated IV curve for SDM.

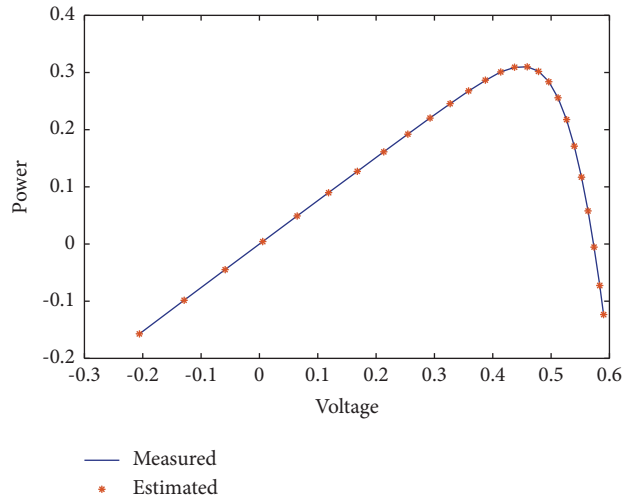

Figure 5: Measured and estimated PV curve for SDM.

Table 4: Comparison of actual and experimental values for DDM.

S. no	I_m	I_e	IAE (current)	V	P_e	P_m	IAE (power)	RE
1	0.763939	0.764	6.14948×10^{-05}	−0.2057	−0.15714	−0.15715	1.26495×10^{-05}	8.04971×10^{-05}
2	0.762582	0.762	0.000582117	−0.1291	−0.09845	−0.09837	7.51513×10^{-05}	−0.00076335
3	0.761337	0.7605	0.000836944	−0.0588	−0.04477	−0.04472	4.92123×10^{-05}	−0.00109931
4	0.760193	0.7605	0.000306786	0.0057	0.004333	0.004335	1.74868×10^{-06}	0.000403563
5	0.759144	0.76	0.000855534	0.0646	0.049041	0.049096	5.52675×10^{-05}	0.001126972
6	0.758172	0.759	0.000828382	0.1185	0.089843	0.089942	9.81633×10^{-05}	0.001092605
7	0.757245	0.757	0.000245333	0.1678	0.127066	0.127025	4.11668×10^{-05}	−0.00032398
8	0.756298	0.757	0.000702222	0.2132	0.161243	0.161392	0.000149714	0.000928499
9	0.755212	0.7555	0.000288146	0.2545	0.192201	0.192275	7.33331×10^{-05}	0.000381543
10	0.753718	0.754	0.000282476	0.2924	0.220387	0.22047	8.2596×10^{-05}	0.000374777
11	0.751334	0.7505	0.000833709	0.3269	0.245611	0.245338	0.00027254	−0.00110964
12	0.747173	0.7465	0.000672634	0.3585	0.267861	0.26762	0.000241139	−0.00090024
13	0.739829	0.7385	0.001329463	0.3873	0.286536	0.286021	0.000514901	−0.00179699
14	0.727118	0.728	0.000881524	0.4137	0.300809	0.301174	0.000364686	0.001212353
15	0.706773	0.7065	0.000273137	0.4373	0.309072	0.308952	0.000119443	−0.00038646
16	0.675302	0.6755	0.000198446	0.459	0.309963	0.310055	9.10868×10^{-05}	0.000293863
17	0.631084	0.632	0.000915506	0.4784	0.301911	0.302349	0.000437978	0.001450687
18	0.572393	0.573	0.000607147	0.496	0.283907	0.284208	0.000301145	0.001060718
19	0.499778	0.499	0.000777945	0.5119	0.255836	0.255438	0.00039823	−0.00155658
20	0.413633	0.413	0.000633148	0.5265	0.217778	0.217445	0.000333353	−0.0015307
21	0.317157	0.3165	0.000657301	0.5398	0.171202	0.170847	0.000354811	−0.00207248
22	0.211867	0.212	0.000133189	0.5521	0.116972	0.117045	7.35338×10^{-05}	0.000628646
23	0.102415	0.1035	0.001084951	0.5633	0.05769	0.058302	0.000611153	0.010593663
24	−0.00948	−0.01	0.000522999	0.5736	−0.00544	−0.00574	0.000299992	0.055186158
25	−0.12436	−0.123	0.001355456	0.5833	−0.07254	−0.07175	0.000790637	−0.01089985
26	−0.20887	−0.21	0.001133954	0.59	−0.12323	−0.1239	0.000669033	0.005429098
IAE (current)			0.016999944		IAE (power)		0.006512664	

5. Results and Discussions

The aim of the paper is to evaluate the SDM of a PV cell's five unmeasured variables (I_{ph}, I_o, R_{Sh}, R_s, and N) and the DDM of a PV cell's seven unmeasured variables (I_{ph}, I_{o1}, I_{o2}, R_{Sh}, R_s, N_1, and $N2$). The AFT algorithm parameters for determining the parameters of the PV model are as follows: maximum iteration = 700; number of thieves (N) = 700; random number (rand, r_1, r_2, and r_4) [0, 1] and $r_3 \geq 0.5$. The configurations for both the lower bound (LB) and upper bound (UB) for SDM, DDM, Photowatt-PWP201, STM6-40/36, and STP6-120/36 cell/module are displayed in Table 1 [38].

5.1. Case Study 1: R. T. C France Solar Cell (Single-Diode Model). Table 2 displays the comparison of actual and experimental values for SDM. Table 3 presents the

Table 5: The IAE, RMSE, and the extracted parameters for DDM.

S. no	Optimization method	IAE (current)	RMSE			I_{ph}	I_{o1}	I_{o2}	R_{Sh}	R_s	N_1	N_2
			Std	Mean	Min							
1	AFT	0.0169	9.52×10^{-06}	7.5×10^{-04}	7.4×10^{-04}	0.7608	0.9999	0.0610	56.4397	0.03783	1.7829	1.3547
2	GSK [27]	0.0297	8.72×10^{-07}	9.8×10^{-04}	9.8×10^{-04}	0.7608	0.2595	0.4791	54.9330	0.0366	1.4627	1.9983
3	DE [27]	0.0228	3.87×10^{-05}	9.9×10^{-04}	9.8×10^{-04}	0.7608	0.3564	0.5762	54.3994	0.0366	1.4575	1.9974
4	GOTLBO [13]	0.0287	9.28×10^{-05}	1.0×10^{-04}	9.8×10^{-04}	0.7608	0.3410	0.2634	54.4147	0.0345	1.4638	1.9910
5	ITLBO [42]	0.0191	1.33×10^{-05}	9.8×10^{-04}	9.8×10^{-04}	0.7608	0.3204	0.8451	53.7216	0.03614	1.4743	1.7892
6	RTLBO [24]	0.0250	1.95×10^{-05}	9.9×10^{-04}	9.8×10^{-04}	0.7608	0.2299	0.8527	49.0850	0.0363	1.4552	1.9614
7	TLABC [39]	0.0197	2.06×10^{-06}	9.8×10^{-04}	9.8×10^{-04}	0.7608	0.4239	0.2401	54.6680	0.0367	1.4567	1.9075
8	HBA [21]	0.02365	1.5022×10^{-07}	9.829×10^{-04}	9.8252×10^{-04}	0.7608	0.2316	0.0000	55.2640	0.0367	1.4530	2.0000
9	IWOA [29]	0.01735	1.9297×10^{-05}	9.9693×10^{-04}	9.8255×10^{-04}	0.7608	0.6771	0.2355	55.4082	0.0367	2.0000	1.4545
10	HBA-OBL [21]	0.02549	1.8757×10^{-07}	9.8283×10^{-04}	9.8254×10^{-04}	0.7608	0.6713	0.0000	55.3172	0.0367	2	1.4545
11	HBO [22]	0.02334	3.8633×10^{-04}	1.563855×10^{-03}	1.04972×10^{-03}	0.7607	0.674	0.197	51.6762	0.0368	1.90873	1.44075
12	WOA [29]	0.01947	1.6685×10^{-03}	3.3497×10^{-03}	1.1293×10^{-03}	0.7611	0.365	0.1274	55.5644	0.0354	1.4970	1.7961

estimated parameters with the RMSE errors from AFT minimum, average, and standard deviation[39]. Figure 3 shows the convergence curves for the formulated objective functions. Figures 4 and 5 display, respectively, the *I-V* and *P-V* properties of a PV cell under real-world and speculative conditions. It is clear from Table 2 that the absolute individual error (IAE) values are less than 3.399×10^{-03} and that the relative error (RE) values range from 6.91×10^{-03} to 2.65897×10^{-01}, proving the SDM's high efficiency as identified by AFT. Furthermore, Table 3 demonstrates that using the proposed AFT algorithm for the SDM provides the minimum RMSE value of 7.72×10^{-04} as compared with the recent MH optimization methods in the literature. Also, it presents the optimal value of the unknown parameters (I_{ph}, I_o, R_{Sh}, R_s, and N) calculated using AFT and other MH optimization methods in the literature as shown in Table 3.

5.2. Case Study II: Double-Diode Model R. T. C France Solar Cell. The values of RE and IAE for both current and power are given in Table 4. Seven parameters (I_{ph}, I_{o1}, I_{o2}, R_{Sh}, R_s, N_1, and N_2) must be evaluated as in the case of DDM, and the estimated parameters along with the minimal level, mean, and standard deviation are shown in Table 5. The converging curve for DDM is shown in Figure 6. The *I-V* and *P-V* curves are shown in Figures 7 and 8. It is clear from Table 4 that IAE values are less than 0.0169 and that the relative error (RE) values range from 8.04971×10^{-05} to 0.055186158, proving the DDM's high efficiency as identified by the AFT method. Also, Table 5 demonstrates that using the proposed AFT algorithm for the DDM provides the minimum RMSE value of 0.00074 as compared with the recent MH optimization methods in the literature.

5.3. Case Study III: STM6-40/36 Monocrystalline PV Module. The Schutten Solar STM6-40/36 PV module is obtained using the AFT technique. It has 36 series-connected polycrystalline cells, each measuring 156 mm in diameter. Twenty data points have been collected at $T = 51^{\circ}C$ for the data set. Table 6 displays the comparison of actual and experimental values for SDM. It is clear from Table 4 that IAE values are less than 0.02179 and that the relative error (RE) values range from −0.00044to 0.001823, proving the DDM's high efficiency as identified by the AFT method. Table 7 shows the results of the parameters acquired by MH optimization techniques in the literature for the STM6-40/36 PV module design. Figures 9–11 depict the convergence, *I-V*, and *P-V* curves to support the overall precision of the derived values. In the operating voltage of both the *I-V* and *P-V* curves, it is clear that the simulated data from the AFT agree well with the observed data. Table 7 also demonstrates that using the proposed AFT algorithm for the STM6-40/36 PV modules provides the minimum RMSE value of 0.001722 as compared with the recent MH optimization methods in the literature. Also, it presents the optimal value of the unknown parameters (I_{ph}, I_o, R_{Sh}, R_s, and N) calculated using AFT and other MH optimization techniques in the literature, as shown in Table 7.

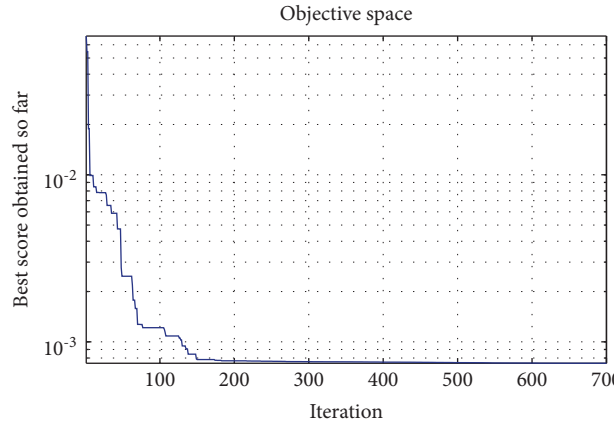

Figure 6: Convergence curve for DDM.

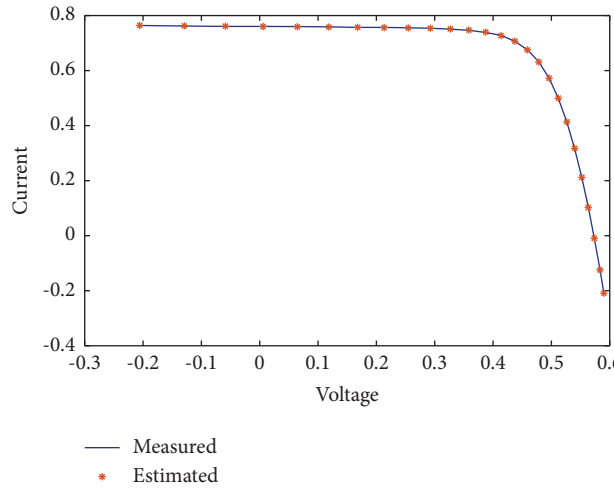

Figure 7: Measured and estimated IV curve for DDM.

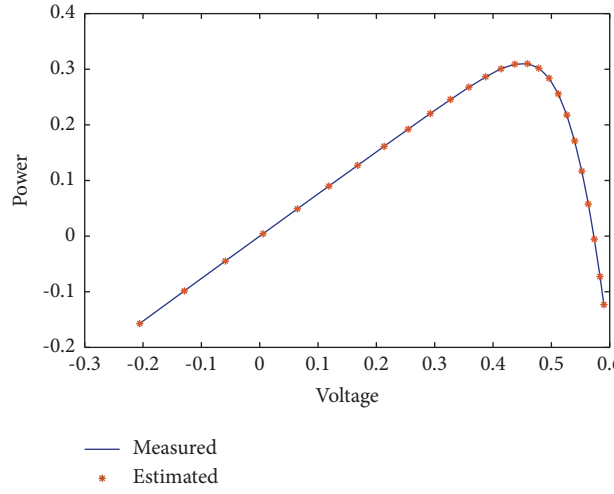

Figure 8: Measured and estimated PV curve for DDM.

Table 6: Comparison of actual and experimental values for the STM6-40/36 module.

S. no	I_m	I_e	IAE (current)	V	P_e	P_m	IAE (power)	RE
1	1.663	1.663458	0.000458	0	0	0	0	0
2	1.663	1.663252	0.000252	0.118	0.196264	0.196234	2.97×10^{-05}	−0.00015
3	1.661	1.659551	0.001449	2.237	3.712416	3.715657	0.003241	0.000872
4	1.653	1.653916	0.000916	5.434	8.987378	8.982402	0.004976	−0.00055
5	1.65	1.650568	0.000568	7.26	11.98312	11.979	0.00412	−0.00034
6	1.645	1.645433	0.000433	9.68	15.92779	15.9236	0.004187	−0.00026
7	1.64	1.639236	0.000764	11.59	18.99874	19.0076	0.008857	0.000466
8	1.636	1.633716	0.002284	12.6	20.58482	20.6136	0.028777	0.001396
9	1.629	1.627289	0.001711	13.37	21.75685	21.77973	0.02288	0.001051
10	1.619	1.618314	0.000686	14.09	22.80205	22.81171	0.009661	0.000424
11	1.597	1.603065	0.006065	14.88	23.85361	23.76336	0.09025	−0.0038
12	1.581	1.581582	0.000582	15.59	24.65686	24.64779	0.009068	−0.00037
13	1.542	1.542323	0.000323	16.4	25.2941	25.2888	0.005305	−0.00021
14	1.524	1.521221	0.002779	16.71	25.41961	25.46604	0.046434	0.001823
15	1.5	1.499202	0.000798	16.98	25.45646	25.47	0.013543	0.000532
16	1.485	1.485268	0.000268	17.13	25.44265	25.43805	0.004595	−0.00018
17	1.465	1.465641	0.000641	17.32	25.3849	25.3738	0.011103	−0.00044
18	1.388	1.387601	0.000399	17.91	24.85193	24.85908	0.007145	0.000287
19	1.118	1.11839	0.00039	19.08	21.33889	21.33144	0.007448	-0.00035
20	0	-2.59×10^{-05}	2.59×10^{-05}	21.02	−0.00055	0	0.000545	0
IAE (current)			0.02179			IAE (power)	0.282165	

Table 7: The IAE, RMSE, and the extracted parameters for STM6-40/36 module.

S.no	Optimization technique	IAE (current)	RMSE			I_{ph}	I_o	R_{Sh}	R_s	N
			Std.	Mean	Min					
1	AFT	0.02179	2.19×10^{-17}	1.722×10^{-03}	1.722×10^{-03}	1.6639	1.7412	573.5339	0.1536	57.9551
2	GSK [27]	0.03949	6.25×10^{-18}	1.7298×10^{-03}	1.7298×10^{-03}	1.6635	1.9240	16.5546	0.0040	1.5315
3	RTLBO [24]	0.0225	2.29×10^{-04}	1.901×10^{-03}	1.7298×10^{-03}	1.6639	1.7024	15.8288	0.0043	1.518
4	TLABC [39]	0.0249	2.04×10^{-04}	2.002×10^{-03}	1.7298×10^{-03}	1.7	1.6338	15.4001	0.005	1.5002
5	BES [40]	0.02486	5.6525×10^{-18}	1.7298×10^{-03}	1.7298×10^{-03}	1.6639	1.7387	15.9283	0.0043	1.5203
6	HBA-OBL [21]	0.0326	1.0079×10^{-08}	1.7298×10^{-03}	1.7298×10^{-03}	1.6639	1.738	573.4188	0.1539	55.7631
7	HBA [21]	0.03648	4.6718×10^{-09}	1.7298×10^{-03}	1.7298×10^{-03}	1.6639	1.7387	573.418	0.1539	55.7631
8	DE [27]	0.0312	2.89×10^{-04}	2.15×10^{-03}	1.7738×10^{-03}	1.6635	2.0741	16.8047	0.0037	1.5395
9	GOTLBO [13]	0.0366	3.41×10^{-04}	2.771×10^{-03}	1.8467×10^{-03}	1.6631	2.3475	17.4323	0.0031	1.5536

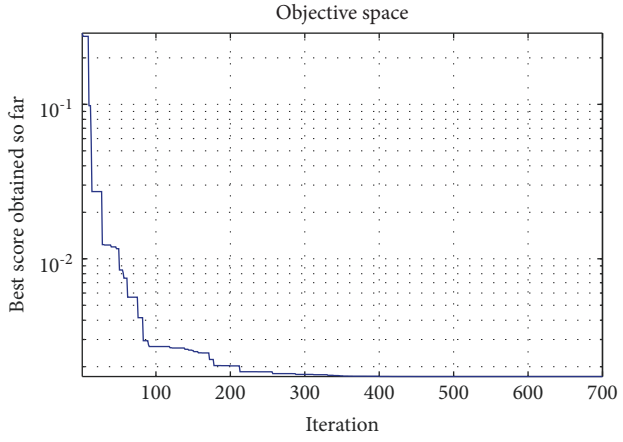

Figure 9: Convergence curve for STM6-40/36.

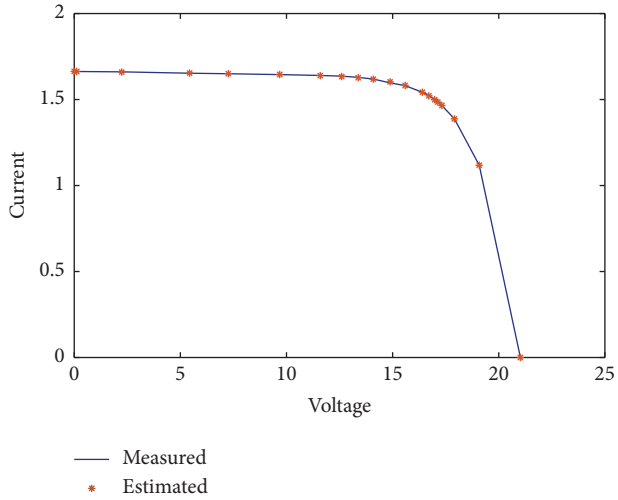

Figure 10: Measured and estimated IV curve for STM6-40/36.

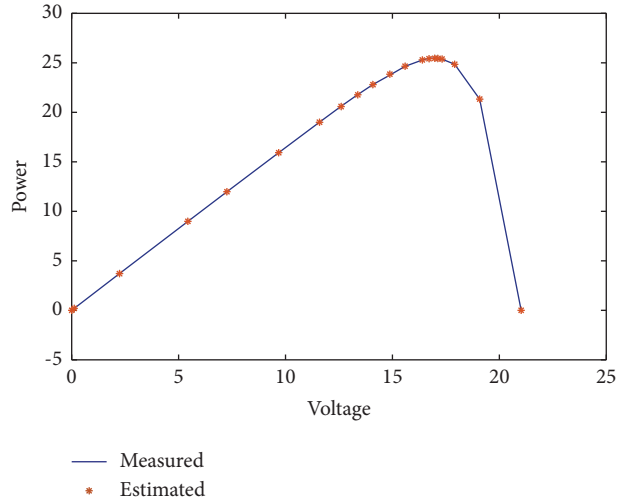

Figure 11: Measured and estimated PV curve for STM6-40/36.

Table 8: Comparison of actual and experimental values for the STP6-120/36 module.

S.no	I_m	I_e	IAE (current)	V	P_e	P_m	IAE (power)	RE
1	7.48	7.472287	0.007713	0	0	0	0	0.001031
2	7.45	7.4501	9.97×10^{-05}	9.06	67.4979	67.497	0.000903	-1.30×10^{-05}
3	7.42	7.446863	0.026863	9.47	70.5218	70.2674	0.254396	−0.00362
4	7.44	7.436659	0.003341	10.32	76.74632	76.7808	0.034478	0.000449
5	7.41	7.418151	0.008151	11.17	82.86074	82.7697	0.091043	−0.0011
6	7.38	7.394243	0.014243	11.81	87.32602	87.1578	0.168216	−0.00193
7	7.37	7.362255	0.007745	12.36	90.99747	91.0932	0.09573	0.001051
8	7.34	7.331017	0.008983	12.74	93.39716	93.5116	0.114441	0.001224
9	7.29	7.284367	0.005633	13.16	95.86226	95.9364	0.074136	0.000773
10	7.23	7.218798	0.011202	13.59	98.10346	98.2557	0.152238	0.001549
11	7.1	7.090271	0.009729	14.17	100.4691	100.607	0.137857	0.00137
12	6.97	6.961243	0.008757	14.58	101.4949	101.6226	0.127681	0.001256
13	6.83	6.818033	0.011967	14.93	101.7932	101.9719	0.178663	0.001752
14	6.58	6.571183	0.008817	15.39	101.1305	101.2662	0.135696	0.00134
15	6.36	6.351667	0.008333	15.71	99.78468	99.9156	0.130916	0.00131
16	6	6.03965	0.03965	16.08	97.11758	96.48	0.637576	−0.00661
17	5.75	5.778132	0.028132	16.34	94.41467	93.955	0.459675	−0.00489
18	5.27	5.273358	0.003358	16.76	88.38148	88.3252	0.056278	−0.00064
19	5.07	5.080897	0.010897	16.9	85.86715	85.683	0.184154	−0.00215
20	4.79	4.783887	0.006113	17.1	81.80448	81.909	0.104524	0.001276
21	4.56	4.543693	0.016307	17.25	78.3787	78.66	0.281298	0.003576
22	4.29	4.270691	0.019309	17.41	74.35273	74.6889	0.336175	0.004501
23	3.83	3.828246	0.001754	17.65	67.56854	67.5995	0.030964	0.000458
24	0	0.00422	0.00422	19.21	0.081073	0	0.081073	0
IAE (current)			0.271318			IAE (power)	3.868108	

5.4. Case Study IV: STP6-120/36 Module. The polycrystalline STP6-120/36 is less than 1000 W/m^2 at 55°C and has 36 series-connected cells. Table 8 shows that the IAE sum is smaller than 4.64×10^{-02}, demonstrating good agreement between the observed and extract values. Table 8 also provides the I_e, I_m, V, P_e,P_m, IAE (current), IAE (power), and RE. The IAE explains the discrepancy between both the observed data and the retrieved value. The findings of various strategies from the literature are also compared in Table 9, with recent MH optimization techniques for the STP6-120/36 PV module design. The comparison proved that AFT is more successful than other MH methods. The RMSE for the AFT application used to extract the PV model's parameters is 0.014451. The analytical findings and convergence curve are displayed in Table 9 and Figure 12. The *I-V* and *P-V* curves of the simulated data discovered by AFT are remarkably compatible with the real data, as shown in Figures 13 and 14. In other terms, when the IAE and RMSE values are low, the obtained values are better (I_{ph}, I_o, R_{Sh}, R_s, and N).

Table 9: The IAE, RMSE, and the extracted parameters for STP6-120/36 module.

S.no.	Optimization techniques	IAE (current)	RMSE			I_{ph}	I_o	R_{Sh}	R_s	N
			Std.	Mean	Min					
1	AFT	0.2713	3.42×10^{-16}	1.4451×10^{-02}	1.4451×10^{-02}	7.4745	1.9158	582.113	0.1691	47.9952
2	HBA [21]	0.3616	1.3247×10^{-05}	1.6601×10^{-02}	1.6016×10^{-02}	7.4725	2.3350	799.9290	0.1654	46.7896
3	HBA-OBL [21]	0.2984	1.3182×10^{-05}	1.6601×10^{-02}	1.6016×10^{-02}	7.4725	2.3350	799.8886	0.1654	46.7896
4	GSK [27]	0.3649	1.44×10^{-16}	1.6601×10^{-02}	1.6601×10^{-02}	7.4725	2.3350	22.2199	0.0046	1.260
5	DE [27]	0.3284	5.13×10^{-03}	2.23×10^{-02}	1.66×10^{-02}	7.4708	2.5614	28.8094	0.0046	1.2657
6	RTLBO [24]	0.2874	8.16×10^{-04}	2.08×10^{-02}	1.66×10^{-02}	7.4728	2.3167	21.6438	0.0046	1.2594
7	GOTLBO [13]	0.365	3.45×10^{-03}	2.16×10^{-02}	1.67×10^{-02}	7.4563	2.2559	22.4749	0.0045	1.2566
8	TLABC [39]	0.2889	5.70×10^{-04}	1.73×10^{-02}	1.67×10^{-02}	7.5611	3.4715	23.6694	0.0049	1.2698
9	BES [40]	0.3303	1.12×10^{-04}	1.69×10^{-02}	1.68×10^{-02}	7.4716	2.3218	23.0265	0.0046	1.2596

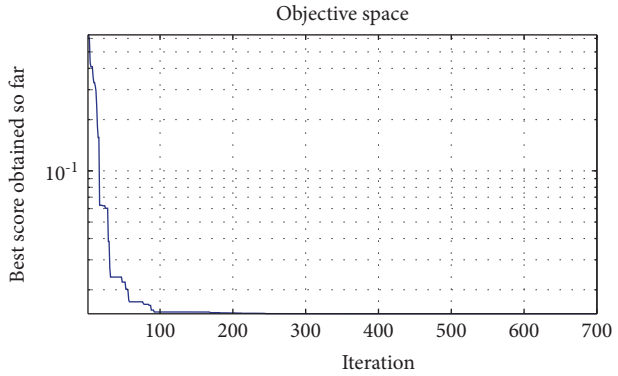

Figure 12: Convergence curve for STP6-120/36.

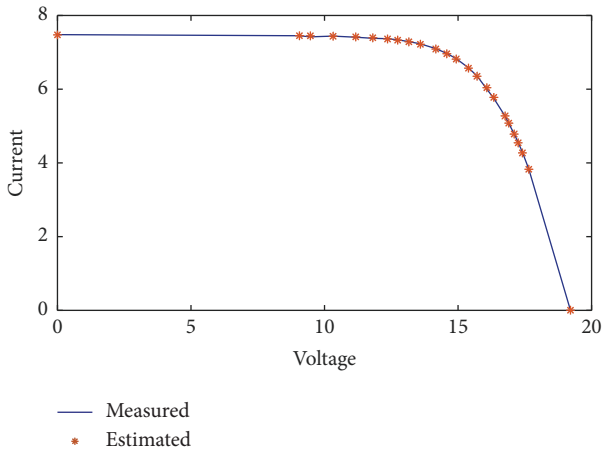

Figure 13: Measured and estimated IV curve for STP6-120/36.

5.5. Case Study V: Photowatt-PWP201 PV Module. The Photowatt-PWP201 PV module, which is made up of 36 silicon cells that are connected and operate under operating conditions of 1000 W/m^2 of solar irradiation and a cell temperature of 45°C, has been used to validate the AFT technique further and demonstrate its effectiveness in estimating the optimal parameters of various models. The outcomes have contrasted with those documented in the literature using other methods. Table 10 is a listing of the outcomes. The findings of additional MH optimization techniques from the literature for the Photowatt-PWP201 PV module design are also compared in Table 11. The comparison proved that AFT is more successful than alternative methods. Better, the RMSE based on the AFT application to extract the PV model's parameters is equivalent to 2.052×10^{-03}. The improved performance observed by AFT for the PV module is obvious from Table 10, where the IAE ratings are lower than 4.418×10^{-03}, and the RE values are between 6.44×10^{-03} and 1.3167×10^{-01}. The analytical findings are shown in Tables 10 and 11, and the convergence curve is shown in Figure 15. The *I-V* and *P-V* curves of the simulated data discovered by AFT are remarkably compatible with the real data, as shown in Figures 16 and 17. Also, it presents the optimal value of the unknown parameters (I_{ph}, I_o, R_{Sh}, R_s, and N) calculated using AFT techniques and other MH optimization techniques in the literature as shown in Table 11.

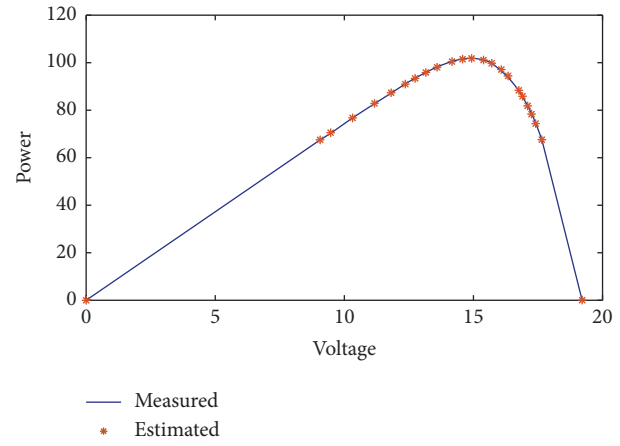

Figure 14: Measured and estimated PV curve for STP6-120/36.

6. Statistical Validations

In this section, the proposed optimization algorithm is statistically tested using a series of separate runs (30) for each case/algorithm using the Friedman and Wilcoxon tests [43, 44]. Tables 12 and 13 show the average rankings for the proposed algorithms using all five solar PV cell/module problems (SDM, DDM, Photowatt-PWP201,

Table 10: Comparison of actual and experimental values for the Photowatt-PWP201 module.

S.no	I_m	I_e	IAE (current)	V	P_e	P_m	IAE (power)	RE
1	1.0315	1.029728	0.0017716	0.1248	0.12851	0.128731	0.000221	0.0017204
2	1.03	1.027661	0.0023389	1.8093	1.859347	1.863579	0.004232	0.002276
3	1.026	1.025725	0.0002755	3.3511	3.437305	3.438229	0.000923	0.0002686
4	1.022	1.023833	0.0018333	4.7622	4.875699	4.866968	0.008731	−0.0017906
5	1.018	1.021814	0.0038136	6.0538	6.185855	6.162768	0.023087	−0.0037322
6	1.0155	1.019323	0.0038229	7.2364	7.376228	7.348564	0.027664	−0.0037505
7	1.014	1.015733	0.0017332	8.3189	8.449783	8.435365	0.014418	−0.0017064
8	1.01	1.009978	2.15×10^{-05}	9.3097	9.402596	9.402797	0.000201	2.13×10^{-05}
9	1.0035	1.000409	0.0030906	10.2163	10.22048	10.25206	0.031575	0.0030894
10	0.988	0.984743	0.0032573	11.0449	10.87638	10.91236	0.035977	0.0033078
11	0.963	0.960189	0.0028113	11.8018	11.33195	11.36513	0.033179	0.0029279
12	0.9255	0.923874	0.0016264	12.4929	11.54186	11.56218	0.020318	0.0017604
13	0.8725	0.873566	0.0010664	13.1231	11.4639	11.4499	0.013995	−0.0012208
14	0.8075	0.808203	0.0007027	13.6983	11.071	11.06138	0.009626	−0.0008695
15	0.7265	0.72855	0.0020499	14.2221	10.36151	10.33236	0.029154	−0.0028137
16	0.6345	0.636633	0.0021332	14.6995	9.35819	9.326833	0.031357	−0.0033508
17	0.5345	0.535427	0.0009272	15.1346	8.103476	8.089444	0.014033	−0.0017317
18	0.4275	0.428198	0.0006983	15.5311	6.65039	6.639545	0.010845	−0.0016307
19	0.3185	0.317849	0.0006513	15.8929	5.051537	5.061889	0.010351	0.0020492
20	0.2085	0.207007	0.0014929	16.2229	3.358255	3.382475	0.024219	0.0072119
21	0.101	0.097645	0.0033547	16.5241	1.613501	1.668934	0.055433	0.0343558
22	−0.008	−0.00859	0.0005907	16.7987	−0.14431	−0.13439	0.009922	−0.0687572
23	−0.111	−0.11097	2.62×10^{-05}	17.0499	−1.89209	−1.89254	0.000447	0.0002361
24	−0.209	−0.20861	0.0003912	17.2793	−3.60461	−3.61137	0.00676	0.0018753
25	−0.303	−0.30093	0.0020724	17.4885	−5.26277	−5.29902	0.036243	0.0068867
IAE (current)			0.0425533		IAE (power)		0.45291	

Table 11: The IAE, RMSE, and the extracted parameters for the Photowatt-PWP201 module.

S.no	Optimization techniques	IAE (current)	RMSE			I_{ph}	I_o	R_{Sh}	R_s	N
			Std	Mean	Min					
1	AFT	0.042553	3.05×10^{-17}	2.052×10^{-03}	2.052×10^{-03}	1.0314	2.6380	821.61	1.2356	49.46379
2	HBA [21]	0.05325	1.6938×10^{-09}	2.4251×10^{-03}	2.4251×10^{-03}	1.0305	3.4823	981.9870	1.2013	48.6428
3	HBA-OBL [21]	0.0525	3.4932×10^{-08}	2.4251×10^{-03}	2.4251×10^{-03}	1.0305	3.4823	981.9831	1.2013	48.6428
4	GSK [27]	0.049932	1.04×10^{-19}	2.4251×10^{-03}	2.4251×10^{-03}	1.0305	3.4823	981.9823 013	1.2013	48.6428
5	DE [27]	0.058921	1.25×10^{-05}	2.4364×10^{-03}	2.4251×10^{-03}	1.0305	3.4823	981.9823	1.2012	48.6848
6	BES [40]	0.0547	2.45×10^{-17}	2.42×10^{-03}	2.425×10^{-03}	1.0305	3.4823	981.9824	1.2013	48.6428
7	GOTLBO [13]	0.062379	7.25×10^{-04}	2.73×10^{-03}	2.43×10^{-03}	1.0305	3.5214	984.656	1.1978	48.686
8	RTLBO [24]	0.056832	4.98×10^{-05}	2.54×10^{-03}	2.43×10^{-03}	1.3030	3.5033	988.5601	1.2006	48.66
9	TLABC [39]	0.0507	1.12×10^{-04}	2.49×10^{-03}	2.43×10^{-03}	1.0306	3.4715	972.9357	1.2017	48.6313

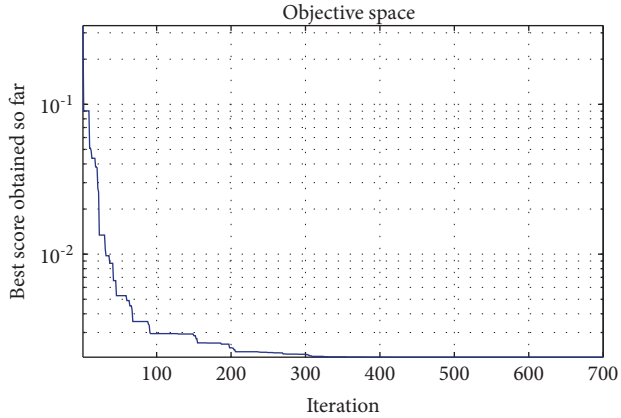

Figure 15: Convergence curve for Photowatt-PWP201.

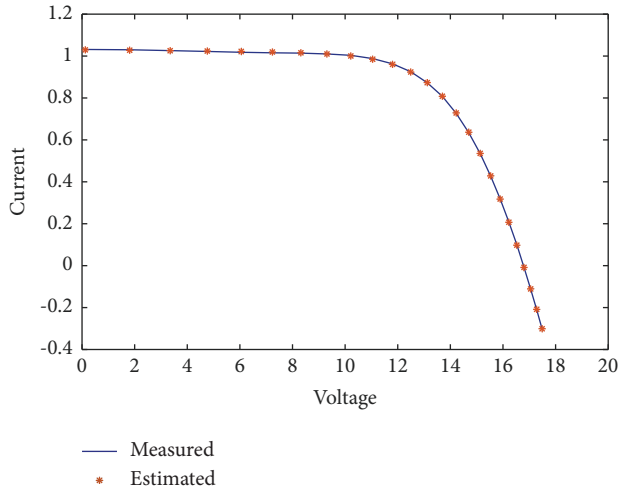

Figure 16: Measured and estimated IV curve for Photowatt-PWP201.

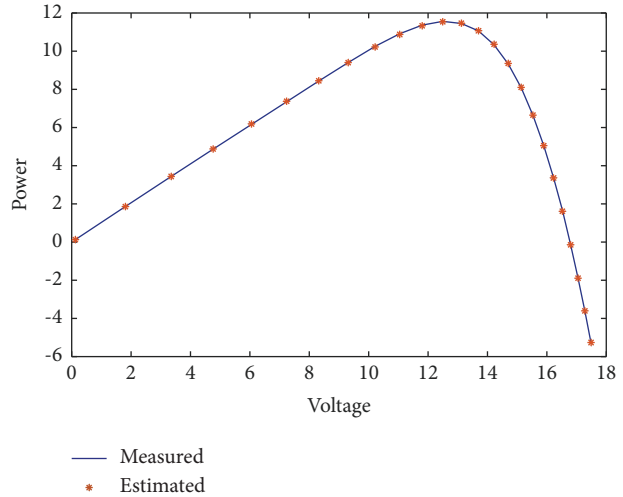

Figure 17: Measured and estimated PV curve for Photowatt-PWP201.

Table 12: Ranking the algorithms based on Friedman's rank for R. T. C France solar cell (SDM and DDM).

Rank	R. T. C France solar cell (SDM)		R. T. C France solar cell (DDM)	
	Algorithm	Friedman's rank	Algorithm	Friedman's rank
1	AFT	1.8235	AFT	1.9706
2	BES	3.4394	HBA	4.7135
3	HBA	3.6318	HBA-OBL	4.731
4	HBA-OBL	4.8769	TLABC	4.9657
5	GSK	6.8577	ITLBO	5.0576
6	TLABC	7.0045	GSK	5.1814
7	IWOA	7.2454	IWOA	7.5452
8	DE	8.1431	RTLBO	7.8467
9	RTLBO	8.2555	DE	8.5058
10	GOTLBO	9.9989	GOTLBO	10.6270
11	HBO	10.1462	HBO	11.4908
12	WOA	11.9971	WOA	12.7316

Table 13: Ranking the algorithms based on Friedman's rank for STM6-40/36, STP6-120/36, and PHOTOWATT-PWP201 MODULEs.

Rank	STM6-40/36 module		STP6-120/36 module		PHOTOWATT-PWP201 module	
	Algorithm	Friedman's rank	Algorithm	Friedman's rank	Algorithm	Friedman's rank
1	AFT	1.9908	AFT	1.7577	AFT	1.9575
2	BES	3.1309	GSK	3.5595	BES	2.8118
3	GSK	3.2481	HBA-OBL	3.5922	GSK	4.3603
4	HBA-OBL	4.4118	HBA	5.0157	HBA	5.3147
5	HBA	5.2469	BES	6.1340	HBA-OBL	5.7725
6	RTLBO	7.4800	TLABC	6.6454	DE	5.9134
7	TLABC	7.4990	RTLBO	7.9825	TLABC	6.8975
8	DE	8.5058	GOTLBO	8.1024	RTLBO	8.2135
9	GOTLBO	8.7603	DE	8.7891	GOTLBO	9.0324

Table 14: Results of the Wilcoxon's rank sum test for R. T. C France solar cell (SDM and DDM).

AFT	R. T. C France solar cell (SDM)				AFT	R. T. C France solar cell (DDM)			
	R^+	R^-	p value	Result		R^+	R^-	p value	Result
BES	465	0	3.0199×10^{-11}	+	GSK	465	0	3.0199×10^{-11}	+
HBA	465	0	3.0180×10^{-11}	+	TLABC	465	0	3.0199×10^{-11}	+
HBA-OBL	465	0	3.0199×10^{-11}	+	ITLBO	465	0	3.0199×10^{-11}	+
GSK	465	0	3.0085×10^{-11}	+	HBA	465	0	3.0199×10^{-11}	+
TLABC	465	0	3.0180×10^{-11}	+	HBA-OBL	465	0	3.0199×10^{-11}	+
IWOA	465	0	3.0199×10^{-11}	+	RTLBO	465	0	3.0199×10^{-11}	+
DE	465	0	3.0199×10^{-11}	+	DE	465	0	3.0199×10^{-11}	+
RTLBO	465	0	3.0180×10^{-11}	+	IWOA	465	0	3.0199×10^{-11}	+
GOTLBO	465	0	3.0199×10^{-11}	+	GOTLBO	465	0	2.9543×10^{-11}	+
HBO	465	0	3.0180×10^{-11}	+	HBO	465	0	3.0199×10^{-11}	+
WOA	465	0	2.9155×10^{-11}	+	WOA	465	0	3.0199×10^{-11}	+

Table 15: Results of the Wilcoxon's rank sum test for STM6-40/36, STP6-120/36, and PHOTOWATT-PWP201 MODULEs.

AFT	STM6-40/36 module				AFT	STP6-120/36 module				AFT	PHOTOWATT-PWP201 module			
	R^+	R^-	p value	Result		R^+	R^-	p value	Result		R^+	R^-	p value	Result
BES	465	0	2.2521×10^{-11}	+	GSK	465	0	1.9418×10^{-11}	+	BES	465	0	2.3936×10^{-11}	+
GSK	465	0	2.2362×10^{-11}	+	HBA-OBL	465	0	2.8574×10^{-11}	+	GSK	465	0	1.2049×10^{-11}	+
HBA-OBL	465	0	2.8039×10^{-11}	+	HBA	465	0	2.8574×10^{-11}	+	HBA	465	0	3.0066×10^{-11}	+
HBA	465	0	2.8305×10^{-11}	+	BES	465	0	2.8574×10^{-11}	+	HBA-OBL	465	0	3.0066×10^{-11}	+
RTLBO	464	1	5.2488×10^{-10}	+	TLABC	465	0	2.8574×10^{-11}	+	DE	465	0	3.0066×10^{-11}	+
TLABC	465	0	2.8305×10^{-11}	+	RTLBO	465	0	2.8556×10^{-11}	+	TLABC	465	0	3.0066×10^{-11}	+
DE	465	0	2.8234×10^{-11}	+	GOTLBO	465	0	2.8574×10^{-11}	+	RTLBO	465	0	3.0066×10^{-11}	+
GOTLBO	465	0	2.8287×10^{-11}	+	DE	465	0	2.8556×10^{-11}	+	GOTLBO	465	0	3.0010×10^{-11}	+

STM6-40/36, and STP6-120/36) based on the Friedman test. The AFT algorithm is shown as the base algorithm. The results verify that the AFT algorithm is superior to other MH algorithms in solving all five solar PV cell/module problems. The results of a statistical analysis utilising Wilcoxon's test comparing AFT and other MH algorithms are summarised in Tables 14 and 15. In general, the performance of AFT is better than other algorithms in all five solar PV cells/modules. In the AFT algorithm versus MH algorithms, the AFT algorithm gets higher $R+$ values than R- in all five solar PV cell/module problems. The results show that the AFT algorithm outperforms existing MH methods in solving all five solar PV cell/module problems.

7. Conclusions and Future Directions

In this paper, a well-known optimization technique, known as the AFT optimization algorithm, is used to obtain the optimum solution for solar PV cells and module parameters. Numerous scenarios have been used for SDM, DDM, and PV panel modules to show the performance of the AFT optimization algorithm. The observed and calculated data's I-V characteristics, as well as P-V characteristics, demonstrate the suggested method's high degree of accuracy. The results of simulation tests and comparisons to other MH optimization techniques illustrate the method's accuracy and validity in extracting the characteristics of a PV cell and module. It offers the benefit of quickly convergent and

consistent results for each test. The approach is presented using real-world information from several solar PV manufacturers (SDM, DDM, Photowatt-PWP201, STM6-40/36, and STP6-120/36). Its accuracy is demonstrated by comparing its RMSE with a variety of MH optimization techniques. As a result, the close similarity between the generated *I-V* and *P-V* curves and the measured features has validated the AFT's accuracy. Furthermore, its application to parameter assessment and to solve the additional power system optimization issues can be used. The statistical validity of the suggested algorithms has been examined using the Friedman and Wilcoxon tests. The suggested AFT algorithm is therefore better than the existing MH optimization algorithms. In the future, hybrid optimization techniques will be used to find out the optimal value of unknown parameters and reduce the RMSE value of solar PV.

Data Availability

The figures and tables used to support the findings of this study are included in the article.

Conflicts of Interest

The authors declare that they have no conflicts of interest.

References

[1] S. Fan, X. Wang, S. Cao, Y. Wang, Y. Zhang, and B. Liu, "A novel model to determine the relationship between dust concentration and energy conversion efficiency of photovoltaic (PV) panels," *Energy*, vol. 252, Article ID 123927, 2022.

[2] S. Fan, W. Liang, G. Wang, Y. Zhang, and S. Cao, "A novel water-free cleaning robot for dust removal from distributed photovoltaic (PV) in water-scarce areas," *Solar Energy*, vol. 241, pp. 553–563, 2022.

[3] P. Lin, S. Cheng, W. Yeh, Z. Chen, and L. Wu, "Parameters extraction of solar cell models using a modified simplified swarm optimization algorithm," *Solar Energy*, vol. 144, pp. 594–603, 2017.

[4] A. Ortiz-Conde, F. J. García Sánchez, and J. Muci, "New method to extract the model parameters of solar cells from the explicit analytic solutions of their illuminated characteristics," *Solar Energy Materials and Solar Cells*, vol. 90, no. 3, pp. 352–361, 2006.

[5] R. Abbassi, A. Abbassi, M. Jemli, and S. Chebbi, "Identification of unknown parameters of solar cell models: a comprehensive overview of available approaches," *Renewable and Sustainable Energy Reviews*, vol. 90, pp. 453–474, 2018.

[6] Y. Li, W. Huang, H. Huang et al., "Evaluation of methods to extract parameters from current voltage characteristics of solar cells," *Solar Energy*, vol. 90, pp. 51–57, 2013.

[7] A. W. Mohamed, A. A. Hadi, and A. K. Mohamed, "Gaining-sharing knowledge based algorithm for solving optimization problems: a novel nature-inspired algorithm," *International Journal of Machine Learning and Cybernetics*, vol. 11, no. 7, pp. 1501–1529, 2020.

[8] J. Kennedy and R. Eberhart, "Particle swarm optimization," in *Proceedings of the ICNN'95 - International Conference on Neural Networks 1995*, vol. 4, pp. 1942–1948, Perth, Australia, November 1995.

[9] R. Ben Messaoud, "Extraction of uncertain parameters of single-diode model of a photovoltaic panel using simulated annealing optimization," *Energy Reports*, vol. 6, pp. 350–357, 2020.

[10] X. Yuan, Y. Xiang, and Y. He, "Parameter extraction of solar cell models using mutative-scale parallel chaos optimization algorithm," *Solar Energy*, vol. 108, pp. 238–251, 2014.

[11] J. P. Ram, T. S. Babu, T. Dragicevic, and N. Rajasekar, "A new hybrid bee pollinator flower pollination algorithm for solar PV parameter estimation," *Energy Conversion and Management*, vol. 135, pp. 463–476, 2017.

[12] A. Askarzadeh and A. Rezazadeh, "Artificial bee swarm optimization algorithm for parameters identification of solar cell models," *Applied Energy*, vol. 102, pp. 943–949, 2013.

[13] X. Chen, K. Yu, W. Du, W. Zhao, and G. Liu, "Parameters identification of solar cell models using generalized oppositional teaching learning based optimization," *Energy*, vol. 99, pp. 170–180, 2016.

[14] D. F. Alam, D. A. Yousri, and M. B. Eteiba, "Flower Pollination Algorithm based solar PV parameter estimation," *Energy Conversion and Management*, vol. 101, pp. 410–422, 2015.

[15] M. S. Ismail, M. Moghavvemi, and T. M. I. Mahlia, "Characterization of PV panel and global optimization of its model parameters using genetic algorithm," *Energy Conversion and Management*, vol. 73, pp. 10–25, 2013.

[16] A. Askarzadeh and A. Rezazadeh, "Parameter identification for solar cell models using harmony search-based algorithms," *Solar Energy*, vol. 86, no. 11, pp. 3241–3249, 2012.

[17] F. Dkhichi, B. Oukarfi, A. Fakkar, and N. Belbounaguia, "Parameter identification of solar cell model using Levenberg Marquardt algorithm combined with simulated annealing," *Solar Energy*, vol. 110, pp. 781–788, 2014.

[18] D. Oliva, E. Cuevas, and G. Pajares, "Parameter identification of solar cells using artificial bee colony optimization," *Energy*, vol. 72, pp. 93–102, 2014.

[19] C. Xiaoping, Q. Bo, and L. Gang, "An application of immune algorithm in FIR filter design," in *Proceedings of the 2003 International Conference on Neural Networks and Signal Processin, 2003*, vol. 1, pp. 473–475, Hong Kong, China, April 2003.

[20] J. Ma, T. O. Ting, K. L. Man, N. Zhang, S. U. Guan, and P. W. H. Wong, "Parameter estimation of photovoltaic models via cuckoo search," *Journal of Applied Mathematics*, vol. 2013, Article ID 362619, 8 pages, 2013.

[21] T. Düzenlı, F. Kutlu Onay, and S. B. Aydemır, "Improved honey badger algorithms for parameter extraction in photovoltaic models," *Optik*, vol. 268, Article ID 169731, 2022.

[22] D. S. AbdElminaam, E. H. Houssein, M. Said, D. Oliva, and A. Nabil, "An efficient heap-based optimizer for parameters identification of modified photovoltaic models," *Ain Shams Engineering Journal*, vol. 13, no. 5, Article ID 101728, 2022.

[23] A. Beşkirli and İ. Dağ, "An efficient tree seed inspired algorithm for parameter estimation of Photovoltaic models," *Energy Reports*, vol. 8, pp. 291–298, 2022.

[24] G. Xiong, J. Zhang, D. Shi, and Y. He, "Parameter identification of solid oxide fuel cells with ranking teaching-learning based algorithm," *Energy Conversion and Management*, vol. 174, pp. 126–137, 2018.

[25] N. Rajasekar, N. Krishna Kumar, and R. Venugopalan, "Bacterial Foraging Algorithm based solar PV parameter estimation," *Solar Energy*, vol. 97, pp. 255–265, 2013.

[26] R. V. Rao, V. J. Savsani, and D. P. Vakharia, "Teaching-Learning-Based Optimization: an optimization method for

continuous non-linear large scale problems," *Information Sciences*, vol. 183, no. 1, pp. 1–15, 2012.

[27] G. Xiong, L. Li, A. W. Mohamed, X. Yuan, and J. Zhang, "A new method for parameter extraction of solar photovoltaic models using gaining sharing knowledge based algorithm," *Energy Reports*, vol. 7, pp. 3286–3301, 2021.

[28] S. Mirjalili and A. Lewis, "The whale optimization algorithm," *Advances in Engineering Software*, vol. 95, pp. 51–67, 2016.

[29] G. Xiong, J. Zhang, D. Shi, and Y. He, "Parameter extraction of solar photovoltaic models using an improved whale optimization algorithm," *Energy Conversion and Management*, vol. 174, pp. 388–405, 2018.

[30] R. Ben Messaoud, "Extraction of uncertain parameters of double-diode model of a photovoltaic panel using Ant Lion Optimization," *SN Applied Sciences*, vol. 2, no. 2, p. 239, 2020.

[31] S. Li, W. Gong, X. Yan et al., "Parameter extraction of photovoltaic models using an improved teaching-learning-based optimization," *Energy Conversion and Management*, vol. 186, pp. 293–305, 2019.

[32] A. A. Cárdenas, M. Carrasco, F. Mancilla-David, A. Street, and R. Cárdenas, "Experimental parameter extraction in the single-diode photovoltaic model via a reduced-space search," *IEEE Transactions on Industrial Electronics*, vol. 64, no. 2, pp. 1468–1476, 2017.

[33] A. Abbassi, R. Gammoudi, M. Ali Dami, O. Hasnaoui, and M. Jemli, "An improved single-diode model parameters extraction at different operating conditions with a view to modeling a photovoltaic generator: a comparative study," *Solar Energy*, vol. 155, pp. 478–489, 2017.

[34] F. J. Toledo and J. M. Blanes, "Geometric properties of the single-diode photovoltaic model and a new very simple method for parameters extraction," *Renewable Energy*, vol. 72, pp. 125–133, 2014.

[35] M. Abdel-Basset, R. Mohamed, R. K. Chakrabortty, K. Sallam, and M. J. Ryan, "An efficient teaching-learning-based optimization algorithm for parameters identification of photovoltaic models: analysis and validations," *Energy Conversion and Management*, vol. 227, Article ID 113614, 2021.

[36] M. Braik, M. H. Ryalat, and H. Al-Zoubi, "A novel meta-heuristic algorithm for solving numerical optimization problems: Ali Baba and the forty thieves," *Neural Computing & Applications*, vol. 34, no. 1, pp. 409–455, 2022.

[37] X. Gao, Y. Cui, J. Hu et al., "Parameter extraction of solar cell models using improved shuffled complex evolution algorithm," *Energy Conversion and Management*, vol. 157, pp. 460–479, 2018.

[38] A. Fathy and H. Rezk, "Parameter estimation of photovoltaic system using imperialist competitive algorithm," *Renewable Energy*, vol. 111, pp. 307–320, 2017.

[39] X. Chen, B. Xu, C. Mei, Y. Ding, and K. Li, "Teaching learning based artificial bee colony for solar photovoltaic parameter estimation," *Applied Energy*, vol. 212, pp. 1578–1588, 2018.

[40] N. F. Nicaire, P. N. Steve, N. E. Salome, and A. O. Grégroire, "Parameter estimation of the photovoltaic system using bald eagle search (BES) algorithm," *International Journal of Photoenergy*, vol. 2021, Article ID 4343203, 20 pages, 2021.

[41] V. J. Chin and Z. Salam, "Coyote optimization algorithm for the parameter extraction of photovoltaic cells," *Solar Energy*, vol. 194, pp. 656–670, 2019.

[42] S. Li, W. Gong, X. Yan et al., "Parameter extraction of photovoltaic models using an improved teaching-learning-based optimization," *Energy Conversion and Management*, vol. 186, pp. 293–305, 2019.

[43] J. Derrac, S. García, D. Molina, and F. Herrera, "A practical tutorial on the use of nonparametric statistical tests as a methodology for comparing evolutionary and swarm intelligence algorithms," *Swarm and Evolutionary Computation*, vol. 1, no. 1, pp. 3–18, Mar 2011.

[44] A. W. Mohamed, A. A. Hadi, and K. M. Jambi, "Novel mutation strategy for enhancing SHADE and LSHADE algorithms for global numerical optimization," *Swarm and Evolutionary Computation*, vol. 50, Article ID 100455, 2019.